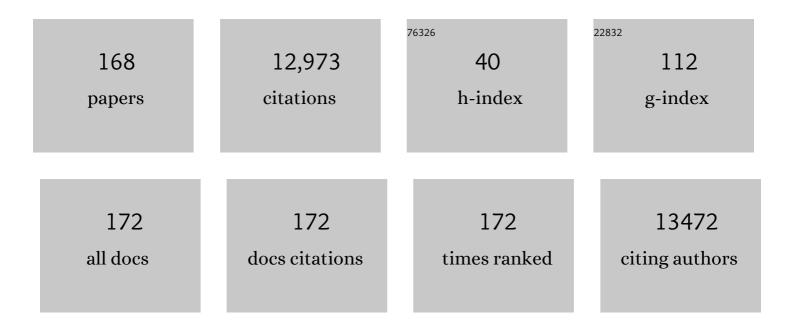
## Takashi Kumasaka

List of Publications by Year in descending order

Source: https://exaly.com/author-pdf/2054614/publications.pdf Version: 2024-02-01



#	Article	IF	CITATIONS
1	Crystal Structure of Rhodopsin: A G Protein-Coupled Receptor. Science, 2000, 289, 739-745.	12.6	5,486
2	Structural basis of glutamate recognition by a dimeric metabotropic glutamate receptor. Nature, 2000, 407, 971-977.	27.8	1,185
3	Self-assembly of tetravalent Goldberg polyhedra from 144 small components. Nature, 2016, 540, 563-566.	27.8	489
4	Structure of the bacterial flagellar protofilament and implications for a switch for supercoiling. Nature, 2001, 410, 331-337.	27.8	480
5	Crystal structure of an orthologue of the NaChBac voltage-gated sodium channel. Nature, 2012, 486, 130-134.	27.8	439
6	Structural Analyses of DNA Recognition by the AML1/Runx-1 Runt Domain and Its Allosteric Control by CBFβ. Cell, 2001, 104, 755-767.	28.9	317
7	<i>In silico</i> discovery of small-molecule Ras inhibitors that display antitumor activity by blocking the Ras–effector interaction. Proceedings of the National Academy of Sciences of the United States of America, 2013, 110, 8182-8187.	7.1	272
8	An oxyl/oxo mechanism for oxygen-oxygen coupling in PSII revealed by an x-ray free-electron laser. Science, 2019, 366, 334-338.	12.6	248
9	Self-Assembly of M 30 L 60 Icosidodecahedron. CheM, 2016, 1, 91-101.	11.7	246
10	Protein encapsulation within synthetic molecular hosts. Nature Communications, 2012, 3, 1093.	12.8	208
11	Small-angle X-ray scattering station at the SPring-8 RIKEN beamline. Journal of Applied Crystallography, 2000, 33, 797-800.	4.5	166
12	<i>ZOO</i> : an automatic data-collection system for high-throughput structure analysis in protein microcrystallography. Acta Crystallographica Section D: Structural Biology, 2019, 75, 138-150.	2.3	156
13	Mechanism of c-Myb–C/EBPβ Cooperation from Separated Sites on a Promoter. Cell, 2002, 108, 57-70.	28.9	155
14	X-ray Structure of β-Carbonic Anhydrase from the Red Alga,Porphyridium purpureum, Reveals a Novel Catalytic Site for CO2 Hydration. Journal of Biological Chemistry, 2000, 275, 5521-5526.	3.4	151
15	Crystal structure of a repair enzyme of oxidatively damaged DNA, MutM (Fpg), from an extreme thermophile,Thermus thermophilusHB8. EMBO Journal, 2000, 19, 3857-3869.	7.8	141
16	Structural Basis for Conformational Dynamics of GTP-bound Ras Protein. Journal of Biological Chemistry, 2010, 285, 22696-22705.	3.4	126
17	Crystal structure of N-carbamyl-d-amino acid amidohydrolase with a novel catalytic framework common to amidohydrolases. Structure, 2000, 8, 729-738.	3.3	122
18	RIKEN structural genomics beamlines at the SPring-8; high throughput protein crystallography with automated beamline operation. Journal of Structural and Functional Genomics, 2006, 7, 15-22	1.2	94

ΤΑΚΑSΗΙ ΚUMASAKA

#	Article	IF	CITATIONS
19	Crystal Structures of 4-α-Glucanotransferase from Thermococcus litoralis and Its Complex with an Inhibitor. Journal of Biological Chemistry, 2003, 278, 19378-19386.	3.4	82
20	Crystal structure of Hfq from Bacillus subtilis in complex with SELEX-derived RNA aptamer: insight into RNA-binding properties of bacterial Hfq. Nucleic Acids Research, 2012, 40, 1856-1867.	14.5	78
21	High-resolution X-ray analysis reveals binding of arginine to aromatic residues of lysozyme surface: implication of suppression of protein aggregation by arginine. Protein Engineering, Design and Selection, 2011, 24, 269-274.	2.1	75
22	Achievement of protein micro-crystallography at SPring-8 beamline BL32XU. Journal of Physics: Conference Series, 2013, 425, 012002.	0.4	72
23	Crystal structure combined with genetic analysis of the Thermus thermophilus ribosome recycling factor shows that a flexible hinge may act as a functional switch. Rna, 2000, 6, 1432-1444.	3.5	70
24	A Norovirus Protease Structure Provides Insights into Active and Substrate Binding Site Integrity. Journal of Virology, 2005, 79, 13685-13693.	3.4	70
25	A nanosecond time-resolved XFEL analysis of structural changes associated with CO release from cytochrome c oxidase. Science Advances, 2017, 3, e1603042.	10.3	68
26	The adoption of a twisted structure of importin-β is essential for the protein-protein interaction required for nuclear transport 1 1Edited by K. Nagai. Journal of Molecular Biology, 2000, 302, 251-264.	4.2	66
27	Crystal structures of the state 1 conformations of the GTPâ€bound Hâ€Ras protein and its oncogenic G12V and Q61L mutants. FEBS Letters, 2012, 586, 1715-1718.	2.8	66
28	Mechanism of metal activation of human hematopoietic prostaglandin D synthase. Nature Structural and Molecular Biology, 2003, 10, 291-296.	8.2	64
29	The 1.55 Ã resolution structure of Nicotiana alata SF11-RNase associated with gametophytic self-incompatibility. Journal of Molecular Biology, 2001, 314, 103-112.	4.2	61
30	Sample management system for a vast amount of frozen crystals at SPring-8. Journal of Applied Crystallography, 2004, 37, 867-873.	4.5	61
31	Beamline Scheduling Software: administration software for automatic operation of the RIKEN structural genomics beamlines at SPring-8. Journal of Synchrotron Radiation, 2005, 12, 380-384.	2.4	60
32	Structural basis of the substrate subsite and the highly thermal stability of xylanase 10B from Thermotoga maritima MSB8. Proteins: Structure, Function and Bioinformatics, 2005, 61, 999-1009.	2.6	59
33	Structural Basis of Leukotriene B4 12-Hydroxydehydrogenase/15-Oxo-prostaglandin 13-Reductase Catalytic Mechanism and a Possible Src Homology 3 Domain Binding Loop. Journal of Biological Chemistry, 2004, 279, 22615-22623.	3.4	58
34	Protein microcrystallography using synchrotron radiation. IUCrJ, 2017, 4, 529-539.	2.2	56
35	The 1.3 à crystal structure of a novel endoâ€Î²â€1,3â€glucanase of glycoside hydrolase family 16 from alkaliphilic <i>Nocardiopsis</i> sp. strain F96. Proteins: Structure, Function and Bioinformatics, 2007, 69, 683-690.	2.6	55
36	A rapid and robust method for selective isotope labeling of proteins. Methods, 2011, 55, 370-378.	3.8	55

Τακάσηι Κυμάσακα

#	Article	IF	CITATIONS
37	The 1.48 à Resolution Crystal Structure of the Homotetrameric Cytidine Deaminase from Mouse‡. Biochemistry, 2006, 45, 7825-7833.	2.5	53
38	Crystal structures of RsbQ, a stress-response regulator in Bacillus subtilis. Protein Science, 2005, 14, 558-565.	7.6	49
39	Structural Insight into Modest Binding of a Non-PXXP Ligand to the Signal Transducing Adaptor Molecule-2 Src Homology 3 Domain. Journal of Biological Chemistry, 2003, 278, 48162-48168.	3.4	47
40	Mail-in data collection at SPring-8 protein crystallography beamlines. Journal of Synchrotron Radiation, 2008, 15, 288-291.	2.4	43
41	Molecular Mechanism for Conformational Dynamics of Ras·GTP Elucidated from In-Situ Structural Transition in Crystal. Scientific Reports, 2016, 6, 25931.	3.3	42
42	Development of a dose-limiting data collection strategy for serial synchrotron rotation crystallography. Journal of Synchrotron Radiation, 2017, 24, 29-41.	2.4	39
43	Structural Basis of the Catalytic Mechanism Operating in Open-Closed Conformers of Lipocalin Type Prostaglandin D Synthase. Journal of Biological Chemistry, 2009, 284, 22344-22352.	3.4	38
44	Structure of a new `aspzincin' metalloendopeptidase fromGrifola frondosa: implications for the catalytic mechanism and substrate specificity based on several different crystal forms. Acta Crystallographica Section D: Biological Crystallography, 2001, 57, 361-368.	2.5	36
45	Improvement of Alkaliphily of <i>Bacillus</i> Alkaline Xylanase by Introducing Amino Acid Substitutions Both on Catalytic Cleft and Protein Surface. Bioscience, Biotechnology and Biochemistry, 2009, 73, 965-967.	1.3	36
46	Trichromatic Concept at SPring-8 RIKEN Beamline I. Journal of Synchrotron Radiation, 1998, 5, 222-225.	2.4	35
47	Humidity control and hydrophilic glue coating applied to mounted protein crystals improves X-ray diffraction experiments. Acta Crystallographica Section D: Biological Crystallography, 2013, 69, 1839-1849.	2.5	35
48	Structural and functional analyses of nucleosome complexes with mouse histone variants TH2a and TH2b, involved in reprogramming. Biochemical and Biophysical Research Communications, 2015, 464, 929-935.	2.1	31
49	Crystal Structures and Enzymatic Properties of a Triamine/Agmatine Aminopropyltransferase from Thermus thermophilus. Journal of Molecular Biology, 2011, 408, 971-986.	4.2	26
50	Upgrade of automated sample exchanger SPACE. Journal of Applied Crystallography, 2012, 45, 234-238.	4.5	25
51	SPring-8 BL41XU, a high-flux macromolecular crystallography beamline. Journal of Synchrotron Radiation, 2013, 20, 910-913.	2.4	25
52	Remote access and automation of SPring-8 MX beamlines. AIP Conference Proceedings, 2016, , .	0.4	23
53	Trichromatic Concept Optimizes MAD Experiments in Synchrotron X-Ray Crystallography. Structure, 2002, 10, 1205-1210.	3.3	22
54	Structural insight of human DEAD-box protein rck/p54 into its substrate recognition with conformational changes. Genes To Cells, 2006, 11, 439-452.	1.2	22

ΤΑΚΑSΗΙ ΚUMASAKA

#	Article	IF	CITATIONS
55	Structure of 2â€deoxyâ€ <i>scyllo</i> â€inosose synthase, a key enzyme in the biosynthesis of 2â€deoxystreptamineâ€containing aminoglycoside antibiotics, in complex with a mechanismâ€based inhibitor and NAD <sup>+</sup> . Proteins: Structure, Function and Bioinformatics, 2008, 70, 517-527.	2.6	22
56	Crystal structure of a family 80 chitosanase from <i>Mitsuaria chitosanitabida</i> . FEBS Letters, 2017, 591, 540-547.	2.8	22
57	Short-lived intermediate in N <sub>2</sub> O generation by P450 NO reductase captured by time-resolved IR spectroscopy and XFEL crystallography. Proceedings of the National Academy of Sciences of the United States of America, 2021, 118, .	7.1	21
58	Cloning, Expression, Crystallization, and Preliminary X-Ray Analysis of Recombinant Mouse Lipocalin-type Prostaglandin D Synthase, a Somnogen-Producing Enzyme. Journal of Biochemistry, 2003, 133, 29-32.	1.7	20
59	Crystal Structures of Blasticidin S Deaminase (BSD). Journal of Biological Chemistry, 2007, 282, 37103-37111.	3.4	19
60	Development of a shutterless continuous rotation method using an X-ray CMOS detector for protein crystallography. Journal of Applied Crystallography, 2009, 42, 1165-1175.	4.5	19
61	Dissection of Hydrogen Bond Interaction Network around an Iron–Sulfur Cluster by Site-Specific Isotope Labeling of Hyperthermophilic Archaeal Rieske-Type Ferredoxin. Journal of the American Chemical Society, 2012, 134, 19731-19738.	13.7	19
62	New micro-beam beamline at SPring-8, targeting at protein micro-crystallography. AIP Conference Proceedings, 2010, , .	0.4	18
63	Structural Features and Functional Dependency on β-Clamp Define Distinct Subfamilies of Bacterial Mismatch Repair Endonuclease MutL. Journal of Biological Chemistry, 2016, 291, 16990-17000.	3.4	17
64	A solute-binding protein in the closed conformation induces ATP hydrolysis in a bacterial ATP-binding cassette transporter involved in the import of alginate. Journal of Biological Chemistry, 2017, 292, 15681-15690.	3.4	16
65	Low-dose X-ray structure analysis of cytochrome <i>c</i> oxidase utilizing high-energy X-rays. Journal of Synchrotron Radiation, 2019, 26, 912-921.	2.4	16
66	Glycine amide shielding on the aromatic surfaces of lysozyme: Implication for suppression of protein aggregation. FEBS Letters, 2011, 585, 555-560.	2.8	15
67	Critical Roles of Interactions among Switch I-preceding Residues and between Switch II and Its Neighboring α-Helix in Conformational Dynamics of the GTP-bound Ras Family Small GTPases. Journal of Biological Chemistry, 2011, 286, 15403-15412.	3.4	14
68	Structural Basis for Polymer Packing and Solvation Properties of the Organogermanium Crystalline Polymer Propagermanium and Its Derivatives. Journal of Pharmaceutical Sciences, 2015, 104, 2482-2488.	3.3	14
69	Analysis of oscillatory rocking curve by dynamical diffraction in protein crystals. Proceedings of the National Academy of Sciences of the United States of America, 2018, 115, 3634-3639.	7.1	13
70	X-ray dose-dependent structural changes of the [2Fe-2S] ferredoxin from Chlamydomonas reinhardtii. Journal of Biochemistry, 2020, 167, 549-555.	1.7	13
71	ISC-like [2Fe–2S] ferredoxin (FdxB) dimer from Pseudomonas putida JCM 20004: structural and electron–nuclear double resonance characterization. Journal of Biological Inorganic Chemistry, 2011, 16, 923-935.	2.6	12
72	Structural analyses of the nucleosome complexes with human testis-specific histone variants, hTh2a and hTh2b. Biophysical Chemistry, 2017, 221, 41-48.	2.8	12

Τακάσηι Κυμάσακα

#	Article	IF	CITATIONS
73	Crystal structure and DNA-binding property of the ATPase domain of bacterial mismatch repair endonuclease MutL from Aquifex aeolicus. Biochimica Et Biophysica Acta - Proteins and Proteomics, 2017, 1865, 1178-1187.	2.3	12
74	Development of SPACE-II for rapid sample exchange at SPring-8 macromolecular crystallography beamlines. Acta Crystallographica Section D: Structural Biology, 2020, 76, 155-165.	2.3	12
75	Resonance Raman characterization of archaeal and bacterial Rieske protein variants with modified hydrogen bond network around the [2Fe-2S] center. Protein Science, 2006, 15, 2019-2024.	7.6	11
76	A Calcium-Dependent Xylan-Binding Domain of Alkaline Xylanase from Alkaliphilic <i>Bacillus</i> sp. Strain 41M-1. Bioscience, Biotechnology and Biochemistry, 2011, 75, 379-381.	1.3	11
77	Structure of Cu/Zn superoxide dismutase from the heavy-metal-tolerant yeast Cryptococcus liquefaciens strain N6. Biochemical and Biophysical Research Communications, 2008, 374, 475-478.	2.1	10
78	Crystal structure of 3-isopropylmalate dehydrogenase in complex with NAD+ and a designed inhibitor. Bioorganic and Medicinal Chemistry, 2009, 17, 7789-7794.	3.0	10
79	Assembly of homogeneous norovirus-like particles accomplished by amino acid substitution. Journal of General Virology, 2011, 92, 2320-2323.	2.9	10
80	Development of an online UV–visible microspectrophotometer for a macromolecular crystallography beamline. Journal of Synchrotron Radiation, 2013, 20, 948-952.	2.4	10
81	<i>In crystallo</i> thermodynamic analysis of conformational change of the topaquinone cofactor in bacterial copper amine oxidase. Proceedings of the National Academy of Sciences of the United States of America, 2019, 116, 135-140.	7.1	10
82	A multiple-CCD X-ray detector and its basic characterization. Journal of Synchrotron Radiation, 1999, 6, 6-18.	2.4	9
83	Cloning and functional characterization of the copper/zinc superoxide dismutase gene from the heavy-metal-tolerant yeast Cryptococcus liquefaciens strain N6. Molecular Genetics and Genomics, 2007, 277, 403-412.	2.1	9
84	Crystallization and preliminary X-ray diffraction studies of the prototypal homologue of mitoNEET ( <i>Tth</i> -NEETOO26) from the extreme thermophile <i>Thermus thermophilus</i> HB8. Acta Crystallographica Section F: Structural Biology Communications, 2008, 64, 1146-1148.	0.7	9
85	Expression, crystallization and preliminary crystallographic analysis of RNA-binding protein Hfq (YmaH) fromBacillus subtilisin complex with an RNA aptamer. Acta Crystallographica Section F: Structural Biology Communications, 2010, 66, 563-566.	0.7	9
86	A temperature-controlled cold-gas humidifier and its application to protein crystals with the humid-air and glue-coating method. Journal of Applied Crystallography, 2019, 52, 699-705.	4.5	9
87	Crystals of ternary protein–DNA complexes composed of DNA-binding domains of c-Myb or v-Myb, C/EBPα or C/EBPĨ² andtom-1A promoter fragment. Acta Crystallographica Section D: Biological Crystallography, 2001, 57, 1655-1658.	2.5	8
88	Structure of the RsbX phosphatase involved in the general stress response of <i>Bacillus subtilis</i> . Acta Crystallographica Section D: Biological Crystallography, 2015, 71, 1392-1399.	2.5	8
89	Structural basis for intramolecular interaction of postâ€ŧranslationally modified Hâ€Ras• <scp>GTP</scp> prepared by protein ligation. FEBS Letters, 2017, 591, 2470-2481.	2.8	8
90	Evaluation of high spatial resolution imaging plate. Nuclear Instruments and Methods in Physics Research, Section A: Accelerators, Spectrometers, Detectors and Associated Equipment, 1998, 416, 314-318.	1.6	7

#	Article	IF	CITATIONS
91	Development of high-speed Imaging Plate detector. Nuclear Instruments and Methods in Physics Research, Section A: Accelerators, Spectrometers, Detectors and Associated Equipment, 2001, 467-468, 1160-1162.	1.6	7
92	Crystallization and preliminary X-ray analyses of quaternary, ternary and binary protein–DNA complexes with involvement of AML1/Runx-1/CBFα Runt domain, CBFβ and the C/EBPβ bZip region. Acta Crystallographica Section D: Biological Crystallography, 2001, 57, 850-853.	2.5	7
93	Crystallization and X-ray analysis of 2-deoxy-scyllo-inosose synthase, the key enzyme in the biosynthesis of 2-deoxystreptamine-containing aminoglycoside antibiotics. Acta Crystallographica Section F: Structural Biology Communications, 2005, 61, 709-711.	0.7	7
94	Unpaired Electron Spin Density Distribution across Reduced [2Fe-2S] Cluster Ligands by <sup>13</sup> C <sub>β</sub> -Cysteine Labeling. Inorganic Chemistry, 2018, 57, 741-746.	4.0	7
95	Evaluation of the data-collection strategy for room-temperature micro-crystallography studied by serial synchrotron rotation crystallography combined with the humid air and glue-coating method. Acta Crystallographica Section D: Structural Biology, 2021, 77, 300-312.	2.3	7
96	Guidelines for <i>de novo</i> phasing using multiple small-wedge data collection. Journal of Synchrotron Radiation, 2021, 28, 1284-1295.	2.4	7
97	Reaction Mechanism and Crystal Structure of 4ALPHAGlucanotransferase from a Hyperthermophilic Archaeon, Thermococcus litoralis Journal of Applied Glycoscience (1999), 2001, 48, 171-175.	0.7	7
98	<i>In situ</i> crystal data-collection and ligand-screening system at SPring-8. Acta Crystallographica Section F, Structural Biology Communications, 2022, 78, 241-251.	0.8	7
99	Crystallization and preliminary crystallographic analysis of endo-1,3-β-glucanase from alkaliphilicNocardiopsisÂsp. strain F96. Acta Crystallographica Section F: Structural Biology Communications, 2006, 62, 20-22.	0.7	6
100	Contribution of salt bridges to alkaliphily of Bacillusalkaline xylanase. Nucleic Acids Symposium Series, 2007, 51, 461-462.	0.3	6
101	Present status of SPring-8 macromolecular crystallography beamlines. AIP Conference Proceedings, 2010, , .	0.4	6
102	Structure of Thermus thermophilus homoisocitrate dehydrogenase in complex with a designed inhibitor. Journal of Biochemistry, 2011, 150, 607-614.	1.7	6
103	SPring-8 BL44XU, beamline designed for structure analysis of large biological macromolecular assemblies. AIP Conference Proceedings, 2016, , .	0.4	6
104	Structural transition of solvated H-Ras/GTP revealed by molecular dynamics simulation and local network entropy. Journal of Molecular Graphics and Modelling, 2017, 77, 51-63.	2.4	6
105	Multiple zinc ions maintain the open conformation of the catalytic site in the <scp>DNA</scp> mismatch repair endonuclease MutL from <i>Aquifex aeolicus</i> . FEBS Letters, 2018, 592, 1611-1619.	2.8	6
106	Synthetic Diamond Monochromator at SPring-8 Review of High Pressure Science and Technology/Koatsuryoku No Kagaku To Gijutsu, 2000, 10, 56-61.	0.0	5
107	Structural Analyses of DNA Recognition by the AML1/Runx-1 Runt Domain and Its Allosteric Control by CBFβ. Cell, 2001, 105, 291.	28.9	5
108	Crystallization and preliminary X-ray studies of xylanase 10B fromThermotoga maritima. Acta Crystallographica Section D: Biological Crystallography, 2003, 59, 1659-1661.	2.5	5

Τακάσηι Κυμασακά

#	Article	IF	CITATIONS
109	Crystallization and X-ray analysis of the N-terminal core domain of a tumour-associated human DEAD-box RNA helicase, rck/p54. Acta Crystallographica Section D: Biological Crystallography, 2004, 60, 156-159.	2.5	5
110	Crystallization and preliminary X-ray diffraction studies of the hyperthermophilic archaeal sulredoxin having the unique Rieske [2Fe–2S] cluster environment. Acta Crystallographica Section D: Biological Crystallography, 2004, 60, 1487-1489.	2.5	5
111	Expression, purification, crystallization and preliminary X-ray analysis of the Met244Ala variant of catalase–peroxidase (KatG) from the haloarchaeonHaloarcula marismortui. Acta Crystallographica Section F: Structural Biology Communications, 2007, 63, 940-943.	0.7	5
112	Crystallization and X-ray analysis of 23â€nm virus-like particles from <i>Norovirus</i> Crystallographica Section F, Structural Biology Communications, 2017, 73, 568-573.	0.8	5
113	Computer-controlled liquid-nitrogen drizzling device for removing frost from cryopreserved crystals. Acta Crystallographica Section F, Structural Biology Communications, 2020, 76, 616-622.	0.8	5
114	A multiple CCD X-ray detector and its first operation with synchrotron radiation X-ray beam. Nuclear Instruments and Methods in Physics Research, Section A: Accelerators, Spectrometers, Detectors and Associated Equipment, 1999, 436, 174-181.	1.6	4
115	The Flexible C-Terminal Region of Aspergillus terreus Blasticidin S Deaminase: Identification of Its Functional Roles with Deletion Enzymes. Biochemical and Biophysical Research Communications, 2002, 290, 421-426.	2.1	4
116	Crystallization and preliminary X-ray diffraction studies of the ISC-like [2Fe–2S] ferredoxin (FdxB) from <i>Pseudomonas putida</i> JCM 20004. Acta Crystallographica Section F: Structural Biology Communications, 2007, 63, 1014-1016.	0.7	4
117	Crystallization and preliminary X-ray analysis of vicenisaminyltransferase VinC. Acta Crystallographica Section F: Structural Biology Communications, 2008, 64, 558-560.	0.7	4
118	Crystallization and preliminary X-ray diffraction studies of hyperthermophilic archaeal Rieske-type ferredoxin (ARF) from <i>Sulfolobus solfataricus</i> P1. Acta Crystallographica Section F: Structural Biology Communications, 2010, 66, 842-845.	0.7	4
119	Glutathione Ethylester, a Novel Protein Refolding Reagent, Enhances both the Efficiency of Refolding and Correct Disulfide Formation. Protein Journal, 2012, 31, 499-503.	1.6	4
120	Alteration of the α1β2/α2β1 subunit interface contributes to the increased hemoglobin-oxygen affinity of high-altitude deer mice. PLoS ONE, 2017, 12, e0174921.	2.5	4
121	Crystallization and preliminary X-ray crystallographic analysis of chitinase F1 (ChiF1) from the alkaliphilicNocardiopsissp. strain F96. Acta Crystallographica Section D: Biological Crystallography, 2004, 60, 2016-2018.	2.5	3
122	Crystallization and preliminary X-ray studies on the reaction center–light-harvesting 1 core complex fromRhodopseudomonas viridis. Acta Crystallographica Section F: Structural Biology Communications, 2005, 61, 83-86.	0.7	3
123	Expression, crystallization and preliminary crystallographic analysis of the PAS domain of RsbP, a stress-response phosphatase from <i>Bacillus subtilis</i> . Acta Crystallographica Section F: Structural Biology Communications, 2009, 65, 559-561.	0.7	3
124	Improvement in Stability of SPring-8 Standard X-Ray Monochromators with Water-Cooled Crystals. AIP Conference Proceedings, 2010, , .	0.4	3
125	Fine-needle capillary mounting for protein microcrystals. Journal of Applied Crystallography, 2012, 45, 785-788.	4.5	3
126	Oncogenic mutations Q61L and Q61H confer active form-like structural features to the inactive state (state 1) conformation of H-Ras protein. Biochemical and Biophysical Research Communications, 2021, 565, 85-90.	2.1	3

Τακάσηι Κυμάσακα

#	Article	IF	CITATIONS
127	Radiation-induced defects in protein crystals observed by X-ray topography. Acta Crystallographica Section D: Structural Biology, 2022, 78, 196-203.	2.3	3
128	Metagenomic mining and structure-function studies of a hyper-thermostable cellobiohydrolase from hot spring sediment. Communications Biology, 2022, 5, 247.	4.4	3
129	Crystal structure of lipocalin-type prostaglandin D synthase. International Congress Series, 2002, 1233, 453-459.	0.2	2
130	Characterization of Nocardiopsis Â-1,3-glucanase with additional carbohydrate-binding domains. Nucleic Acids Symposium Series, 2007, 51, 459-460.	0.3	2
131	Crystallization and preliminary crystallographic analysis of the complex between triiodothyronine and thebb′ fragment of rat protein disulfide isomerase. Acta Crystallographica Section F: Structural Biology Communications, 2012, 68, 476-478.	0.7	2
132	A convenient tool for gas derivatization using fine-needle capillary mounting for protein crystals. Journal of Synchrotron Radiation, 2013, 20, 999-1002.	2.4	2
133	3D Manipulation of Protein Microcrystals with Optical Tweezers for X-ray Crystallography. Journal of Physics: Conference Series, 2013, 425, 012011.	0.4	2
134	A Lynch syndrome-associated mutation at a Bergerat ATP-binding fold destabilizes the structure of the DNA mismatch repair endonuclease MutL. Journal of Biological Chemistry, 2020, 295, 11643-11655.	3.4	2
135	Automated data-processing system for multiple small-wedge data. Acta Crystallographica Section A: Foundations and Advances, 2017, 73, a335-a335.	0.1	2
136	Crystallization and Preliminary X-Ray Study of H2-Proteinase from the Venom of Trimeresurus flavoviridis. Journal of Biochemistry, 1995, 117, 929-930.	1.7	1
137	High Throughput Protein Crystallography at RIKEN Structural Genomic Beamlines. AIP Conference Proceedings, 2004, , .	0.4	1
138	Crystallization and preliminary X-ray analysis of the stress-response PPM phosphatase RsbX fromBacillus subtilis. Acta Crystallographica Section F: Structural Biology Communications, 2009, 65, 1128-1130.	0.7	1
139	Crystallization and preliminary X-ray analysis of isopentenyl diphosphate isomerase fromMethanocaldococcus jannaschii. Acta Crystallographica Section F: Structural Biology Communications, 2011, 67, 101-103.	0.7	1
140	Crystal structures of a subunit of the formylglycinamide ribonucleotide amidotransferase, PurS, fromThermus thermophilus,Sulfolobus tokodaiiandMethanocaldococcus jannaschii. Acta Crystallographica Section F, Structural Biology Communications, 2016, 72, 627-635.	0.8	1
141	Construction of a supramolecule comprising [2,3,9,10,16,17,23,24-octakis(2,6-dimethylphenoxy)phthalocyaninato]zinc(II) and (5,10,15,20-tetraphenylporphyrinato)zinc(II). IUCrData, 2018, 3, .	0.3	1
142	Trichromatic Concept for Rapid Protein Crystallographic Analysis. Seibutsu Butsuri, 2001, 41, 156-159.	0.1	1
143	Current status of protein micro-crystallography at SPring-8. Acta Crystallographica Section A: Foundations and Advances, 2014, 70, C333-C333.	0.1	1
144	SHIKA: a fast and accurate spot finder for raster scan on microfocus beamlines. Acta Crystallographica Section A: Foundations and Advances, 2014, 70, C352-C352.	0.1	1

ΤΑΚΑSΗΙ ΚUMASAKA

#	Article	IF	CITATIONS
145	<title>Performance of multiple-CCD x-ray detector system at SPring-8 for protein&lt;br&gt;crystallography</title> . , 1999, , .		0
146	Prospects for X-ray Crystal Structure Analysis of Selenoproteins with SPring-8 Synchrotron Radiation Journal of Health Science, 2000, 46, 426-429.	0.9	0
147	An unexpected gift from fungicide metabolism studies: blasticidin S deaminase (BSD) from Aspergillus terreus. Progress in Biotechnology, 2002, , 55-60.	0.2	Ο
148	Crystallization and preliminary X-ray diffraction studies of a hyperthermophilic Rieske protein variant (SDX-triple) with an engineered rubredoxin-like mononuclear iron site. Acta Crystallographica Section F: Structural Biology Communications, 2006, 62, 993-995.	0.7	0
149	SPring-8 Structural Biology Beamlines / Automatic Beamline Operation at RIKEN Structural Genomics Beamlines. AIP Conference Proceedings, 2007, , .	0.4	0
150	Automated system for data collection and data processing using microcrystals. Acta Crystallographica Section A: Foundations and Advances, 2015, 71, s187-s187.	0.1	0
151	Chemo-mechanical Coupling Mechanism of Rotation of Mammalian F1-ATPase by Static and Dynamic X-ray Crystallographic Studies. Biochimica Et Biophysica Acta - Bioenergetics, 2018, 1859, e83.	1.0	0
152	Upgrade of bending magnet MX beamline BL38B1 at SPring-8. AIP Conference Proceedings, 2019, , .	0.4	0
153	Novel Insights into the Structural Perturbation Induced by the Oncogenic Mutations, Q61L and Q61H, in Ras State 1. Biophysical Journal, 2020, 118, 42a.	0.5	0
154	Introduction to Software for Protein Crystallography Nihon Kessho Gakkaishi, 2000, 42, 474-477.	0.0	0
155	Development of Structure Analysis by MAD Method Nihon Kessho Gakkaishi, 2003, 45, 14-18.	0.0	0
156	Crystallographic analysis of the PAS domain of RsbP, a stress-response phosphatase inBacillus subtilis. Acta Crystallographica Section A: Foundations and Advances, 2009, 65, s140-s140.	0.3	0
157	Protein Crystal Mounting Method by Using Humid Air and Hydrophobic Polymer Coating. Nihon Kessho Gakkaishi, 2014, 56, 194-200.	0.0	0
158	Upgrade of a high flux MX beamline BL41XU at SPring-8. Acta Crystallographica Section A: Foundations and Advances, 2014, 70, C331-C331.	0.1	0
159	IPR Beamline for Macromolecular Assemblies at SPring-8 (BL44XU). Acta Crystallographica Section A: Foundations and Advances, 2014, 70, C1684-C1684.	0.1	0
160	Processing of Protein Crystals using by Deep-UV Pulsed Laser. Acta Crystallographica Section A: Foundations and Advances, 2014, 70, C334-C334.	0.1	0
161	A new protein crystal mounting method using humid air and glue coating. Acta Crystallographica Section A: Foundations and Advances, 2014, 70, C1146-C1146.	0.1	0
162	Experimental phasing with serial crystallography at XFEL and synchrotron radiation. Acta Crystallographica Section A: Foundations and Advances, 2016, 72, s21-s21.	0.1	0

#	Article	IF	CITATIONS
163	Fixed-target serial crystallography at SACLA. Acta Crystallographica Section A: Foundations and Advances, 2017, 73, a341-a341.	0.1	ο
164	Development of data collections of SPring-8 MX beamlines. Acta Crystallographica Section A: Foundations and Advances, 2017, 73, C642-C642.	0.1	0
165	Low-dose X-ray structure analysis of cytochrome oxidase utilizing high-energy X-rays. Acta Crystallographica Section A: Foundations and Advances, 2017, 73, C1027-C1027.	0.1	Ο
166	Fixed-targets serial crystallography at SPring-8 and SACLA. Acta Crystallographica Section A: Foundations and Advances, 2018, 74, a337-a337.	0.1	0
167	Present status of SPring-8 macromolecular crystallography beamlines. Acta Crystallographica Section A: Foundations and Advances, 2018, 74, e175-e175.	0.1	Ο
168	Remodeling of the optics for a micro-focusing protein crystallography beamline at SPring-8. , 2019, , .		0